

Pros and Cons of the Bethe-Salpeter Formalism for Ground-State Energies

Pierre-François Loos,^{1,*} Anthony Scemama,^{1,†} Ivan Duchemin,^{2,‡} Denis Jacquemin,^{3,§} and Xavier Blase^{4,¶}

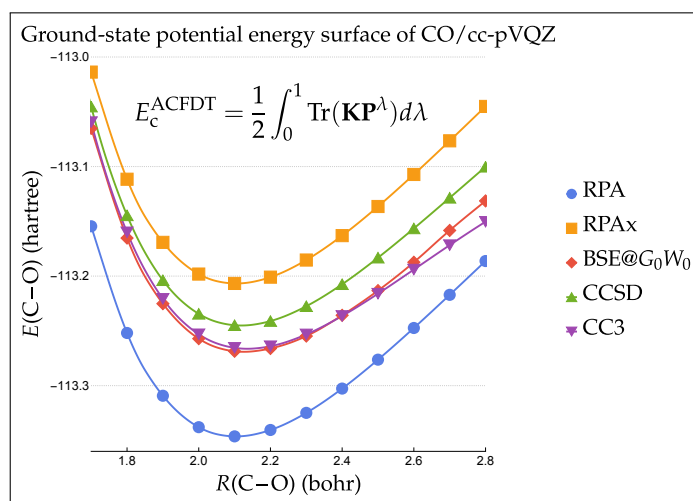
¹Laboratoire de Chimie et Physique Quantiques (UMR 5626), Université de Toulouse, CNRS, UPS, France

²Université Grenoble Alpes, CEA, IRIG-MEM-L Sim, 38054 Grenoble, France

³Laboratoire CEISAM - UMR CNRS 6230, Université de Nantes, 2 Rue de la Houssinière, BP 92208, 44322 Nantes Cedex 3, France

⁴Université Grenoble Alpes, CNRS, Institut NEEL, F-38042 Grenoble, France

The combination of the many-body Green's function GW approximation and the Bethe-Salpeter equation (BSE) formalism has shown to be a promising alternative to time-dependent density-functional theory (TD-DFT) for computing vertical transition energies and oscillator strengths in molecular systems. The BSE formalism can also be employed to compute ground-state correlation energies thanks to the adiabatic-connection fluctuation-dissipation theorem (ACFDT). Here, we study the topology of the ground-state potential energy surfaces (PES) of several diatomic molecules near their equilibrium bond length. Thanks to comparisons with state-of-art computational approaches (CC3), we show that ACFDT@BSE is surprisingly accurate, and can even compete with lower-order coupled cluster methods (CC2 and CCSD) in terms of total energies and equilibrium bond distances for the considered systems. However, we sometimes observe unphysical irregularities on the ground-state PES in relation with difficulties in the identification of a few GW quasiparticle energies.



With a similar computational scaling as time-dependent density-functional theory (TD-DFT),^{1,2} the many-body Green's function Bethe-Salpeter equation (BSE) formalism³⁻⁸ is a valuable alternative that has gained momentum in the past few years for studying molecular systems.⁹⁻²¹ It now stands as a cost-effective computational method that can model excited states^{22,23} with a typical error of 0.1–0.3 eV for spin-conserving transitions according to large and systematic benchmarks.²⁴⁻³⁰ One of the main advantages of BSE compared to TD-DFT is that it allows a faithful description of charge-transfer states.³¹⁻³⁶ Moreover, when performed on top of a (partially) self-consistent $evGW$ calculation,³⁷⁻⁴³ BSE@ $evGW$ has been shown to be weakly dependent on its starting point (*e.g.*, on the exchange-correlation functional selected for the underlying DFT calculation).^{24,43} However, similar to adiabatic TD-DFT,⁴⁴⁻⁴⁷ the static version of BSE cannot describe multiple excitations.⁴⁸⁻⁵⁰

A significant limitation of the BSE formalism, as compared to TD-DFT, lies in the lack of analytical nuclear gradients (*i.e.*, the first derivatives of the energy with respect to the nu-

clear displacements) for both the ground and excited states,⁵¹ preventing efficient studies of excited-state processes (*e.g.*, chemoluminescence and fluorescence) associated with geometric relaxation of ground and excited states, and structural changes upon electronic excitation.⁵²⁻⁵⁵ While calculations of the GW quasiparticle energy ionic gradients is becoming increasingly popular,⁵⁶⁻⁶¹ only one pioneering study of the excited-state BSE gradients has been published so far.⁶² In this seminal work devoted to small molecules (CO and NH₃), only the BSE excitation energy gradients were calculated, while computing the Kohn-Sham (KS) LDA forces as its ground-state contribution.

In contrast to TD-DFT which relies on KS-DFT⁶³⁻⁶⁵ as its ground-state analog, the ground-state BSE energy is not a well-defined quantity, and no clear consensus has been found regarding its formal definition. Consequently, the BSE ground-state formalism remains in its infancy with very few available studies for atomic and molecular systems.⁶⁶⁻⁶⁹ In the largest available benchmark study⁶⁷ encompassing the total energies of the atoms H–Ne, the atomization energies of the 26 small

molecules forming the HEAT test set,⁷⁰ and the bond lengths and harmonic vibrational frequencies of 3d transition-metal monoxides, the BSE correlation energy, as evaluated within the adiabatic-connection fluctuation-dissipation theorem (ACFDT) framework,⁷¹ was mostly discarded from the set of tested techniques due to instabilities (negative frequency modes in the BSE polarization propagator) and replaced by an approximate (RPAsX) approach where the screened-Coulomb potential matrix elements was removed from the resonant electron-hole contribution.^{67,72} Such a modified BSE polarization propagator was inspired by a previous study on the homogeneous electron gas (HEG).⁷² Within RPAsX, amounting to neglect excitonic effects in the electron-hole propagator, the question of using either KS-DFT or *GW* eigenvalues in the construction of the propagator becomes further relevant, increasing accordingly the number of possible definitions for the ground-state correlation energy. Finally, renormalizing or not the Coulomb interaction by the interaction strength λ in the Dyson equation for the interacting polarizability (see below) leads to two different versions of the BSE correlation energy,⁶⁷ emphasizing further the lack of general agreement around the definition of the ground-state BSE energy.

Here, in analogy to the random-phase approximation (RPA)-type formalisms^{73–77} and similarly to Refs. 66, 67, and 72, the ground-state BSE energy is calculated in the adiabatic connection framework. Embracing this definition, the purpose of the present Letter is to investigate the quality of ground-state PES near equilibrium obtained within the BSE approach for several diatomic molecules. The location of the minimum on the ground-state PES is of particular interest. This study is a first necessary step towards the development of analytical nuclear gradients within the BSE@*GW* formalism. Thanks to comparisons with both similar and state-of-art computational approaches, we show that the ACFDT@BSE@*GW* approach is surprisingly accurate, and can even compete with high-order coupled cluster (CC) methods in terms of absolute energies and equilibrium distances. However, we also observe that, in some cases, unphysical irregularities on the ground-state PES, which are due to the appearance of a satellite resonance with a weight similar to that of the *GW* quasiparticle peak.^{78–82}

In order to compute the neutral (optical) excitations of the system and their associated oscillator strengths, the BSE expresses the two-body propagator^{4,83}

$$L(1, 2, 1', 2') = L_0(1, 2, 1', 2') + \int d3d4d5d6L_0(1, 4, 1', 3)\Xi(3, 5, 4, 6)L(6, 2, 5, 2') \quad (1)$$

as the linear response of the one-body Green's function G with respect to a general non-local external potential

$$\Xi(3, 5, 4, 6) = i \frac{\delta[v_H(3)\delta(3, 4) + \Sigma_{xc}(3, 4)]}{\delta G(6, 5)}, \quad (2)$$

which takes into account the self-consistent variation of the Hartree potential

$$v_H(1) = -i \int d2v(2)G(2, 2^+), \quad (3)$$

(where v is the bare Coulomb operator) and the exchange-correlation self-energy Σ_{xc} . In Eq. (1), $L_0(1, 2, 1', 2') = -iG(1, 2')G(2, 1')$, and $(1) = (\mathbf{r}_1, \sigma_1, t_1)$ is a composite index gathering space, spin and time variables. In the *GW* approximation,^{83–87} we have

$$\Sigma_{xc}^{GW}(1, 2) = iG(1, 2)W(1^+, 2), \quad (4)$$

where W is the screened Coulomb operator, and hence the BSE reduces to

$$\Xi(3, 5, 4, 6) = \delta(3, 4)\delta(5, 6)v(3, 6) - \delta(3, 6)\delta(4, 5)W(3, 4), \quad (5)$$

where, as commonly done, we have neglected the term $\delta W/\delta G$ in the functional derivative of the self-energy.^{88–90} Finally, the static approximation is enforced, *i.e.*, $W(1, 2) = W(\{\mathbf{r}_1, \sigma_1, t_1\}, \{\mathbf{r}_2, \sigma_2, t_2\})\delta(t_1 - t_2)$, which corresponds to restricting W to its static limit, *i.e.*, $W(1, 2) = W(\{\mathbf{r}_1, \sigma_1\}, \{\mathbf{r}_2, \sigma_2\}; \omega = 0)$.

For a closed-shell system in a finite basis, to compute the singlet BSE excitation energies (within the static approximation) of the physical system (*i.e.*, $\lambda = 1$), one must solve the following linear response problem^{2,83,91}

$$\begin{pmatrix} \mathbf{A}^\lambda & \mathbf{B}^\lambda \\ -\mathbf{B}^\lambda & -\mathbf{A}^\lambda \end{pmatrix} \begin{pmatrix} \mathbf{X}_m^\lambda \\ \mathbf{Y}_m^\lambda \end{pmatrix} = \Omega_m^\lambda \begin{pmatrix} \mathbf{X}_m^\lambda \\ \mathbf{Y}_m^\lambda \end{pmatrix}, \quad (6)$$

where Ω_m^λ is the m th excitation energy with eigenvector $(\mathbf{X}_m^\lambda \mathbf{Y}_m^\lambda)^\top$ at interaction strength λ , \top is the matrix transpose, and we assume real-valued spatial orbitals $\{\phi_p(\mathbf{r})\}_{1 \leq p \leq N}$. The matrices \mathbf{A}^λ , \mathbf{B}^λ , \mathbf{X}^λ , and \mathbf{Y}^λ are all of size $OV \times OV$ where O and V are the number of occupied and virtual orbitals (*i.e.*, $N = O + V$ is the total number of spatial orbitals), respectively. In the following, the index m labels the OV single excitations, i and j are occupied orbitals, a and b are unoccupied orbitals, while p , q , r , and s indicate arbitrary orbitals.

In the absence of instabilities (*i.e.*, when $\mathbf{A}^\lambda - \mathbf{B}^\lambda$ is positive-definite),⁹¹ Eq. (6) is usually transformed into an Hermitian eigenvalue problem of smaller dimension

$$(\mathbf{A}^\lambda - \mathbf{B}^\lambda)^{1/2}(\mathbf{A}^\lambda + \mathbf{B}^\lambda)(\mathbf{A}^\lambda - \mathbf{B}^\lambda)^{1/2}\mathbf{Z}_m^\lambda = (\Omega_m^\lambda)^2\mathbf{Z}_m^\lambda, \quad (7)$$

where the excitation amplitudes are

$$(\mathbf{X}^\lambda + \mathbf{Y}^\lambda)_m = (\Omega_m^\lambda)^{-1/2}(\mathbf{A}^\lambda - \mathbf{B}^\lambda)^{1/2}\mathbf{Z}_m^\lambda, \quad (8a)$$

$$(\mathbf{X}^\lambda - \mathbf{Y}^\lambda)_m = (\Omega_m^\lambda)^{+1/2}(\mathbf{A}^\lambda - \mathbf{B}^\lambda)^{-1/2}\mathbf{Z}_m^\lambda. \quad (8b)$$

Introducing the so-called Mulliken notation for the bare two-electron integrals

$$(pq|rs) = \iint \frac{\phi_p(\mathbf{r})\phi_q(\mathbf{r})\phi_r(\mathbf{r}')\phi_s(\mathbf{r}')}{|\mathbf{r} - \mathbf{r}'|} d\mathbf{r}d\mathbf{r}', \quad (9)$$

and the corresponding (static) screened Coulomb potential matrix elements at coupling strength λ

$$W_{pq,rs}^\lambda = \iint \phi_p(\mathbf{r})\phi_q(\mathbf{r})W^\lambda(\mathbf{r}, \mathbf{r}')\phi_r(\mathbf{r}')\phi_s(\mathbf{r}')d\mathbf{r}d\mathbf{r}', \quad (10)$$

the BSE matrix elements read

$$A_{ia,jb}^{\lambda,BSE} = \delta_{ij}\delta_{ab}(\epsilon_a^{GW} - \epsilon_i^{GW}) + \lambda[2(ia|jb) - W_{ij,ab}^\lambda], \quad (11a)$$

$$B_{ia,jb}^{\lambda,BSE} = \lambda[2(ia|bj) - W_{ib,aj}^\lambda], \quad (11b)$$

where ϵ_p^{GW} are the *GW* quasiparticle energies. In the standard BSE approach, W^λ is built within the direct RPA scheme, *i.e.*,

$$W^\lambda(\mathbf{r}, \mathbf{r}') = \int \frac{\epsilon_\lambda^{-1}(\mathbf{r}, \mathbf{r}''; \omega = 0)}{|\mathbf{r}' - \mathbf{r}''|} d\mathbf{r}'', \quad (12a)$$

$$\epsilon_\lambda(\mathbf{r}, \mathbf{r}'; \omega) = \delta(\mathbf{r} - \mathbf{r}') - \lambda \int \frac{\chi_0(\mathbf{r}, \mathbf{r}''; \omega)}{|\mathbf{r}' - \mathbf{r}''|} d\mathbf{r}'', \quad (12b)$$

with ϵ_λ the dielectric function at coupling constant λ and χ_0 the non-interacting polarizability. In the occupied-to-virtual orbital product basis, the spectral representation of W^λ can be written as follows in the case of real spatial orbitals

$$W_{ij,ab}^\lambda(\omega) = (ij|ab) + 2 \sum_m^{OV} [ij|m][ab|m] \times \left(\frac{1}{\omega - \Omega_m^{\lambda, \text{RPA}} + i\eta} - \frac{1}{\omega + \Omega_m^{\lambda, \text{RPA}} - i\eta} \right), \quad (13)$$

where the spectral weights at coupling strength λ read

$$[pq|m] = \sum_i^O \sum_a^V (pq|ia)(\mathbf{X}_m^\lambda + \mathbf{Y}_m^\lambda)_{ia}. \quad (14)$$

In the case of complex orbitals, we refer the reader to Ref. 92 for a correct use of complex conjugation in the spectral representation of W .

In Eq. (13), η is a positive infinitesimal, and $\Omega_m^{\lambda, \text{RPA}}$ are the direct (*i.e.*, without exchange) RPA neutral excitation energies computed by solving the linear eigenvalue problem (6) with the following matrix elements

$$A_{ia,jb}^{\lambda, \text{RPA}} = \delta_{ij}\delta_{ab}(\epsilon_a^{\text{HF}} - \epsilon_i^{\text{HF}}) + 2\lambda(ia|jb), \quad (15a)$$

$$B_{ia,jb}^{\lambda, \text{RPA}} = 2\lambda(ia|bj), \quad (15b)$$

where ϵ_p^{HF} are the Hartree-Fock (HF) orbital energies.

The relationship between the BSE formalism and the well-known RPax (*i.e.*, RPA with exchange) approach can be obtained by switching off the screening so that W^λ reduces to the bare Coulomb potential v . In this limit, the *GW* quasiparticle energies reduce to the HF eigenvalues, and Eqs. (11a) and (11b) to the RPax equations:

$$A_{ia,jb}^{\lambda, \text{RPax}} = \delta_{ij}\delta_{ab}(\epsilon_a^{\text{HF}} - \epsilon_i^{\text{HF}}) + \lambda[2(ia|jb) - (ij|ab)], \quad (16a)$$

$$B_{ia,jb}^{\lambda, \text{RPax}} = \lambda[2(ia|bj) - (ib|aj)]. \quad (16b)$$

The key quantity to define in the present context is the total BSE ground-state energy E^{BSE} . Although this choice is not unique,⁶⁷ we propose here to define it as

$$E^{\text{BSE}} = E^{\text{nuc}} + E^{\text{HF}} + E_c^{\text{BSE}}, \quad (17)$$

where E^{nuc} and E^{HF} are the nuclear repulsion energy and electronic ground-state HF energy (respectively), and

$$E_c^{\text{BSE}} = \frac{1}{2} \int_0^1 \text{Tr}(\mathbf{K}\mathbf{P}^\lambda) d\lambda \quad (18)$$

is the ground-state BSE correlation energy computed in the adiabatic connection framework, where

$$\mathbf{K} = \begin{pmatrix} \tilde{\mathbf{A}}^{\lambda=1} & \mathbf{B}^{\lambda=1} \\ \mathbf{B}^{\lambda=1} & \tilde{\mathbf{A}}^{\lambda=1} \end{pmatrix} \quad (19)$$

is the interaction kernel^{67,76} [with $\tilde{A}_{ia,jb}^\lambda = \lambda(ia|bj)$],

$$\mathbf{P}^\lambda = \begin{pmatrix} \mathbf{Y}^\lambda(\mathbf{Y}^\lambda)^\top & \mathbf{Y}^\lambda(\mathbf{X}^\lambda)^\top \\ \mathbf{X}^\lambda(\mathbf{Y}^\lambda)^\top & \mathbf{X}^\lambda(\mathbf{X}^\lambda)^\top \end{pmatrix} - \begin{pmatrix} \mathbf{0} & \mathbf{0} \\ \mathbf{0} & \mathbf{1} \end{pmatrix} \quad (20)$$

is the correlation part of the two-electron density matrix at interaction strength λ , and Tr denotes the matrix trace. Note that the present definition of the BSE correlation energy [see Eq. (18)], which we refer to as BSE@*GW*@HF in the following, has been named ‘‘XBS’’ for ‘‘extended Bethe Salpeter’’ by Holzer *et al.*⁶⁷ In contrast to DFT where the electron density is fixed along the adiabatic path, in the present formalism, the density is not maintained as λ varies. Therefore, an additional contribution to Eq. (18) originating from the variation of the Green’s function along the adiabatic connection should be, in principle, added. However, as commonly done within RPA and RPax,^{67,74,75} we shall neglect it in the present study.

Equation (18) can also be straightforwardly applied to RPA and RPax, the only difference being the expressions of \mathbf{A}^λ and \mathbf{B}^λ used to obtain the eigenvectors \mathbf{X}^λ and \mathbf{Y}^λ entering in the definition of \mathbf{P}^λ [see Eq. (20)]. For RPA, these expressions have been provided in Eqs. (15a) and (15b), and their RPax analogs in Eqs. (16a) and (16b). In the following, we will refer to these two types of calculations as RPA@HF and RPax@HF, respectively. Finally, we will also consider the RPA@*GW*@HF scheme which consists in replacing the HF orbital energies in Eq. (15a) by the *GW* quasiparticles energies.

Note that, for spin-restricted closed-shell molecular systems around their equilibrium geometry (such as the ones studied here), one rarely encounters singlet instabilities as these systems can be classified as weakly correlated. However, singlet instabilities may appear in the presence of strong correlation, *e.g.*, when the bonds are stretched, hampering in particular the calculation of atomization energies.⁶⁷ Even for weakly correlated systems, triplet instabilities are much more common, but triplet excitations do not contribute to the correlation energy in the ACFDT formulation.^{74–76}

All the *GW* calculations performed to obtain the screened Coulomb operator and the quasiparticle energies are done using a (restricted) HF starting point, which is an adequate choice in the case of the (small) systems that we have considered here. Perturbative *GW* (or G_0W_0)^{37,93} calculations are employed as starting points to compute the BSE neutral excitations. In the case of G_0W_0 , the quasiparticle energies are obtained by linearizing the frequency-dependent quasiparticle equation. Further details about our implementation of G_0W_0 can be found in Refs. 80 and 81. Finally, the infinitesimal η is set to zero for all calculations. The numerical integration required to compute the correlation energy along the adiabatic path [see Eq. (18)] is performed with a 21-point Gauss-Legendre quadrature. Comparison with the so-called plasmon (or trace) formula⁷³ at the RPA level has confirmed the excellent accuracy of this quadrature scheme over λ .

For comparison purposes, we have also computed the PES at the second-order Møller-Plesset perturbation theory (MP2), as well as with various increasingly accurate CC methods, namely, CC2⁹⁴, CCSD,⁹⁵ and CC3.⁹⁶ These calculations have been performed with DALTON⁹⁷ and PSI4.⁹⁸ The computational cost of these methods, in their usual implementation, scale as $O(N^5)$, $O(N^5)$, $O(N^6)$, and $O(N^7)$, respectively. As shown in Refs. 99 and 100, CC3 provides extremely accurate ground-state (and excited-state) geometries, and will be taken as reference in the present study. All the other calculations have been performed with our locally developed *GW* software.^{80,81} As one-electron basis sets, we employ the Dunning family (cc-pVXZ) defined with cartesian Gaussian functions. Unless otherwise stated, the frozen-core approximation is not applied in order to provide a fair comparison between methods. We have, however, found that our conclusions hold within the frozen-core approximation (see the [supporting information](#) for information).

Because Eq. (18) requires the entire BSE singlet excitation spectrum for each quadrature point, we perform several complete diagonalization of the $OV \times OV$ BSE linear response matrix [see Eq. (7)], which corresponds to a $O(O^3V^3) = O(N^6)$ computational cost. This step is, by far, the computational bottleneck in our current implementation. However, we are currently pursuing different avenues to lower the formal scaling and practical cost of this step by computing the two-electron density matrix of Eq. (20) via a quadrature in frequency space.^{82,101}

In order to illustrate the performance of the BSE-based adiabatic connection formulation, we compute the ground-state PES of several closed-shell diatomic molecules around their equilibrium geometry: H₂, LiH, LiF, HCl, N₂, CO, BF, and F₂. The PES of these molecules are represented in Figs. 1, 2, 3, and 4, while the computed equilibrium distances and correlation energies are gathered in Table I. Both of these properties are computed with Dunning’s cc-pVQZ basis set. Graphs and tables for the corresponding double- and triple- ζ basis sets can be found in the [supporting information](#).

Let us start with the two smallest molecules, H₂ and LiH. Their PES computed with the cc-pVQZ basis are reported in Fig. 1. For H₂, we take as reference the full configuration interaction (FCI) energies¹⁰² and we also report the MP2 curve and its third-order variant (MP3), which improves upon MP2 towards FCI. RPA@HF and RPA@G₀W₀@HF yield almost identical results, and both significantly overestimate the FCI correlation energy, while RPAx@HF and BSE@G₀W₀@HF slightly over- and undershoot the FCI energy, respectively, RPAx@HF yielding the best match to FCI in the case of H₂. Interestingly, the BSE@G₀W₀@HF scheme yields a more accurate equilibrium bond length than any other method irrespectively of the basis set (see Table in the [supporting information](#)). For example, BSE@G₀W₀@HF/cc-pVQZ is only off by 0.003 bohr as compared to FCI/cc-pVQZ, while RPAx@HF, MP2, and CC2 underestimate the bond length by 0.008, 0.011, and 0.011 bohr, respectively. The RPA-based schemes are much less accurate, with even shorter equilibrium bond lengths. This is a general trend that is magnified in larger systems as the ones discussed below.

Despite the shallow nature of its PES, the scenario is al-

most identical for LiH for which we report the CC2, CCSD and CC3 energies in addition to MP2 energies. In this case, RPAx@HF and BSE@G₀W₀@HF nestle the CCSD and CC3 energy curves, these surfaces running almost perfectly parallel to one another. Here again, the BSE@G₀W₀@HF/cc-pVQZ equilibrium bond length is extremely accurate (3.017 bohr) as compared to CC3/cc-pVQZ (3.019 bohr).

The cases of LiF and HCl (see Fig. 2) are chemically interesting as they correspond to strongly polarized bonds towards the halogen atoms which are much more electronegative than the first-column elements. For these partially ionic bonds, the performance of BSE@G₀W₀@HF is terrific with an almost perfect match to the CC3 curve. Maybe surprisingly, BSE@G₀W₀@HF is on par with both CC2 and CCSD, and outperforms RPAx@HF by a big margin, the latter fact being also observed for the other diatomics discussed below. Interestingly, while CCSD and CC2 systematically underestimates the total energy, the BSE@G₀W₀@HF energy is always lower than the reference CC3 energy. This observation is not only true for LiF and HCl, but holds for every single systems that is considered herein. Moreover, this is consistent with the study by Maggio and Kresse on the HEG showing that BSE slightly overestimates the correlation energy as compared to QMC reference data.⁷² Similarly, the much larger overestimation of the correlation energy that we observe at the RPA@*GW* level was also observed for the HEG. Care must be taken however in drawing comparisons since the HEG study of Ref. 72 was performed starting with LDA eigenstates.

For HCl, the data reported in Table I show that the BSE@G₀W₀@HF equilibrium bond length is again in very good agreement with its CC3 counterpart as it underestimates the bond lengths by a few hundredths of bohr only. However, in the case of LiF, the attentive reader can observe a small “glitch” in the *GW*-based curves very close to their minimum. As observed in Refs. 78–80 and explained in details in Refs. 81 and 82, these irregularities, which makes particularly tricky the location of the minima, are due to “jumps” between distinct solutions of the *GW* quasiparticle equation. Including a broadening via an increase of the η value entering in the expression of the *GW* self-energy and the screened Coulomb operator softens the problem, but does not remove it completely. When irregularities are present in the PES, we have fitted a Morse potential of the form $M(R) = D_0 \left\{ 1 - \exp[-\alpha(R - R_{eq})] \right\}^2$ to the PES in order to provide an estimate of the equilibrium bond length. These values are reported in parenthesis in Table I. For the smooth PES where one can obtain both the genuine minimum and the fitted minimum (*i.e.*, based on the Morse curve), this procedure has been shown to be very accurate with an error of the order of 10^{-3} bohr in most cases. We note that these irregularities are much smaller than the differences between the BSE and the other RPA-like techniques (RPA, RPAx, RPA@*GW*) leaving BSE unambiguously more accurate than these approaches.

Let us now look at the isoelectronic series N₂, CO, and BF, which have a decreasing bond order (from triple to single bond). The conclusions drawn for the previous systems also apply to these molecules. In particular, as shown in Fig. 3, the performance of BSE@G₀W₀@HF is outstanding with an error of the

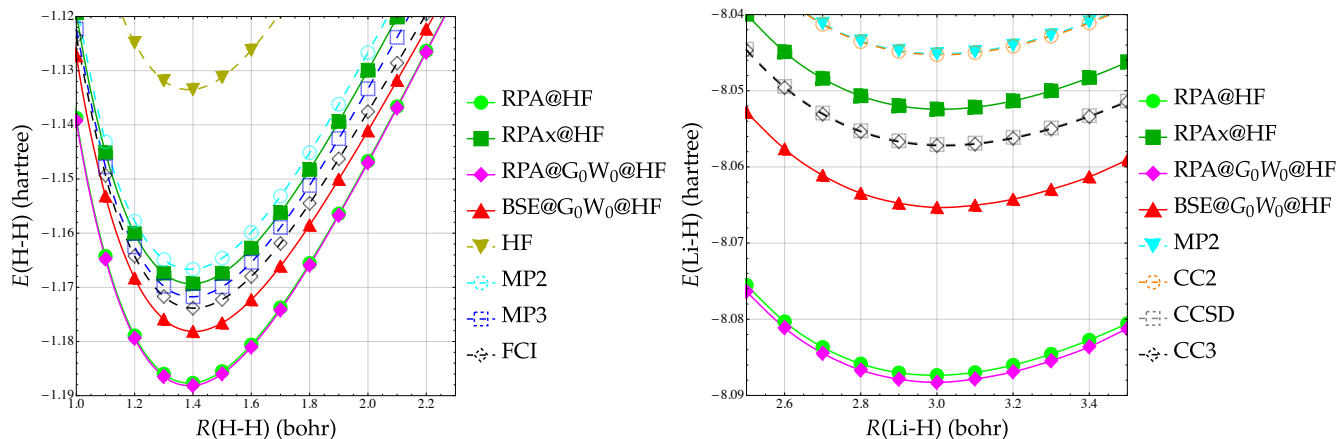


FIG. 1. Ground-state PES of H_2 (left) and LiH (right) around their respective equilibrium geometry obtained at various levels of theory with the cc-pVQZ basis set.

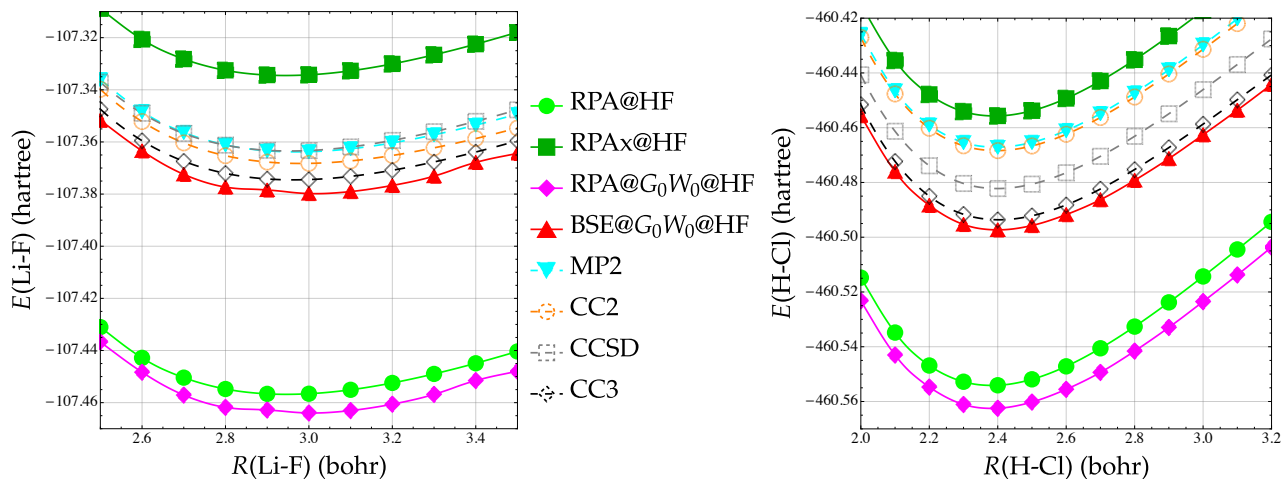


FIG. 2. Ground-state PES of LiF (left) and HCl (right) around their respective equilibrium geometry obtained at various levels of theory with the cc-pVQZ basis set.

order of 1% on the correlation energy. Importantly, it systematically outperforms both CC2 and CCSD. One can notice some irregularities in the PES of BF with the cc-pVDZ et cc-pVTZ basis sets (see the [supporting information](#)). The PES of N_2 and CO are smooth though, and yield accurate equilibrium bond lengths once more. Indeed, at the $BSE@G_0W_0@HF/cc-pVQZ$ level of theory, we obtain 2.065, 2.134, and 2.385 bohr for N_2 , CO , and BF , respectively, which has to be compared with the CC3/cc-pVQZ values of 2.075, 2.136 and 2.390 bohr, respectively.

As a final example, we consider the F_2 molecule, a notoriously difficult case to treat due to the weakness of its covalent bond (see Fig. 4), hence its relatively long equilibrium bond length (2.663 bohr at the CC3/cc-pVQZ level). Similarly to what is observed for LiF and BF , there are irregularities near the minimum of the G_0W_0 -based curves. However, $BSE@G_0W_0@HF$ is the closest to the CC3 curve, with an error on the correlation energy of 1% and an estimated bond length of 2.640 bohr (via a Morse fit) at the $BSE@G_0W_0@HF/cc-$

pVQZ level. Note that, for this system, triplet (and then singlet) instabilities appear for quite short bond lengths. However, around the equilibrium structure, we have not encountered any instabilities. This is an important outcome of the present study as the difficulties encountered at large interatomic distances (*i.e.*, close to the dissociation limit) do not prevent the BSE approach to be potentially useful and accurate in the vicinity of equilibrium distances. Furthermore, preliminary calculations could not detect any singlet instabilities in the vicinity of the lowest singlet excited-state minima.

As a final remark, we would like to mention that although we have considered here only a limited set of compounds, our correlation energy mean absolute error (MAE) with $BSE@G_0W_0@HF$ of 5.5 mHa (as compared to CC3) is significantly smaller than the one obtained with MP2, CC2, and CCSD (18.2, 13.1 and 13.5 mHa respectively). For comparison, the RPA-related formalisms return larger MAEs of 75.6, 43.1, and 68.2 mHa for $BSE@G_0W_0@HF$, $RPAx@HF$, and $RPA@HF$, respectively.

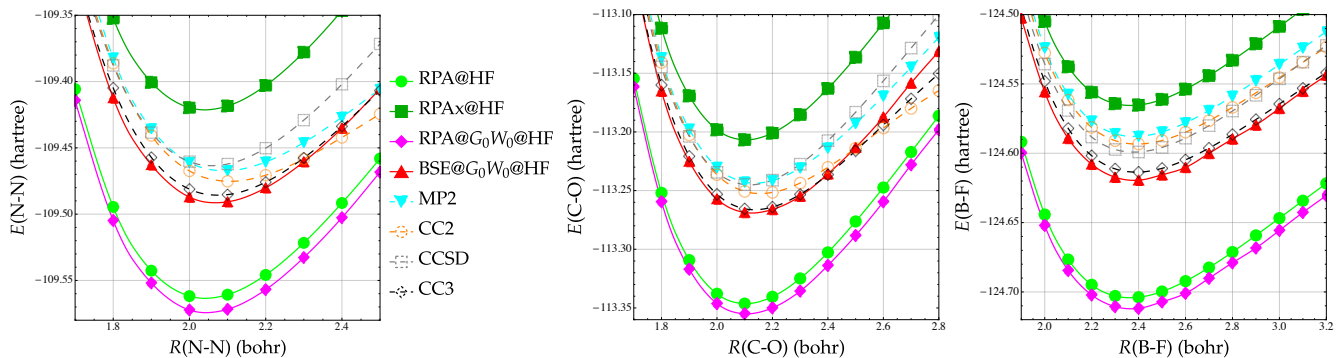


FIG. 3. Ground-state PES of the isoelectronic series N_2 (left), CO (center), and BF (right) around their respective equilibrium geometry obtained at various levels of theory with the cc-pVQZ basis set.

TABLE I. Equilibrium bond length R_{eq} (in bohr) and correlation energy E_c (in millihartree) for the ground state of diatomic molecules obtained with the cc-pVQZ basis set at various levels of theory. For each system and each method, the correlation energy is computed at its respective equilibrium bond length (*i.e.*, $R = R_{eq}$). When irregularities appear in the PES, the R_{eq} values are reported in parenthesis and they have been obtained by fitting a Morse potential to the PES. The error (in %) compared to the reference CC3 values are reported in square brackets.

Method	Equilibrium bond length R_{eq} (bohr)							
	H_2	LiH	LiF	HCl	N_2	CO	BF	F_2
CC3	1.402	3.019	2.963	2.403	2.075	2.136	2.390	2.663
CCSD	1.402[+0.0%]	3.020[+0.0%]	2.953[-0.3%]	2.398[-0.2%]	2.059[-0.8%]	2.118[-0.8%]	2.380[-0.4%]	2.621[-1.6%]
CC2	1.391[-0.8%]	2.989[-1.0%]	2.982[+0.6%]	2.396[-0.3%]	2.106[+1.5%]	2.156[+0.9%]	2.393[+0.1%]	2.665[+0.1%]
MP2	1.391[-0.8%]	3.008[-0.4%]	2.970[+0.2%]	2.395[-0.3%]	2.091[+0.8%]	2.137[+0.1%]	2.382[-0.3%]	2.634[-1.1%]
BSE@ G_0W_0 @HF	1.399[-0.2%]	3.017[-0.1%]	(2.974)[+0.4%]	2.400[-0.1%]	2.065[-0.5%]	2.134[-0.1%]	2.385[-0.2%]	(2.640)[-0.9%]
RPA@ G_0W_0 @HF	1.382[-1.4%]	2.997[-0.7%]	(2.965)[+0.1%]	2.370[-1.5%]	2.043[-1.5%]	2.132[-0.2%]	2.365[-1.1%]	(2.571)[-3.5%]
RPAx@HF	1.394[-0.6%]	3.011[-0.3%]	2.944[-0.6%]	2.391[-0.5%]	2.041[-1.6%]	2.104[-1.5%]	2.366[-1.0%]	2.565[-3.7%]
RPA@HF	1.386[-1.1%]	2.994[-0.8%]	2.946[-0.6%]	2.382[-0.9%]	2.042[-1.6%]	2.103[-1.5%]	2.364[-1.1%]	2.573[-3.4%]

Method	Correlation energy $-E_c$ (millihartree)							
	H_2	LiH	LiF	HCl	N_2	CO	BF	F_2
CC3	40.4	70.0	383.7	382.2	494.4	477.6	447.5	668.9
CCSD	40.4[+0.0%]	69.8[-0.2%]	372.6[-2.9%]	370.8[-3.0%]	470.6[-4.8%]	455.2[-4.7%]	432.9[-3.3%]	644.0[-3.7%]
CC2	33.3[-17.6%]	57.3[-18.1%]	376.7[-1.8%]	356.9[-6.6%]	488.0[-1.3%]	465.5[-2.5%]	427.3[-4.5%]	654.9[-2.1%]
MP2	33.2[-17.9%]	57.9[-17.2%]	373.0[-2.8%]	355.7[-6.9%]	478.0[-3.3%]	455.0[-4.7%]	421.6[-5.8%]	644.3[-3.7%]
BSE@ G_0W_0 @HF	46.5[+15.2%]	78.1[+11.6%]	388.9[+1.4%]	385.9[+1.0%]	499.1[+1.0%]	481.2[+0.8%]	453.1[+1.3%]	675.7[+1.0%]
RPA@ G_0W_0 @HF	57.6[+42.6%]	101.1[+44.5%]	473.1[+23.3%]	451.2[+18.1%]	580.3[+17.4%]	566.5[+18.6%]	545.5[+21.9%]	794.3[+18.8%]
RPAx@HF	37.9[-6.2%]	65.2[-6.8%]	343.6[-10.5%]	344.2[-9.9%]	427.2[-13.6%]	416.3[-12.8%]	399.1[-10.8%]	586.1[-12.4%]
RPA@HF	57.3[+42.0%]	100.2[+43.2%]	465.9[+21.4%]	442.7[+15.8%]	569.4[+15.2%]	555.9[+16.4%]	537.7[+20.2%]	781.3[+16.8%]

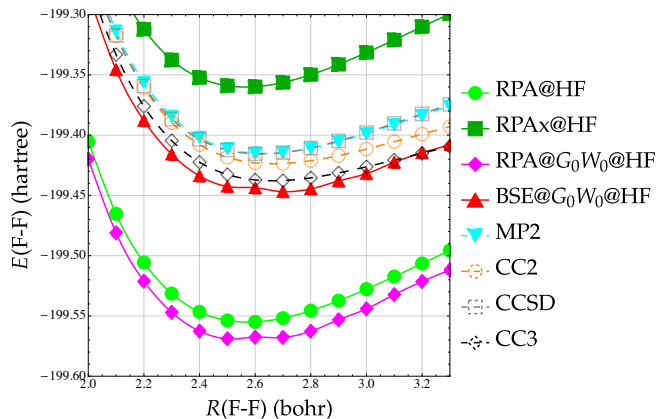


FIG. 4. Ground-state PES of F_2 around its equilibrium geometry obtained at various levels of theory with the cc-pVQZ basis set.

In this Letter, we hope to have illustrated that the ACFDT@BSE formalism is a promising methodology for the computation of accurate ground-state PES and their corre-

sponding equilibrium structures. To do so, we have shown that calculating the BSE correlation energy computed within the ACFDT framework yields extremely accurate PES around equilibrium. We have illustrated this for 8 diatomic molecules for which we have also computed reference ground-state energies using coupled cluster methods (CC2, CCSD, and CC3). For the larger systems considered here, we have observed that BSE@ G_0W_0 recovers 99% of the CC3 correlation energy. Moreover, because triplet states do not contribute to the ACFDT correlation energy and singlet instabilities do not appear for weakly-correlated systems around their equilibrium structure, the present scheme does not suffer from singlet nor triplet instabilities. However, we have also observed that, in some cases, unphysical irregularities on the ground-state PES due to the appearance of discontinuities as a function of the bond length for some of the GW quasiparticle energies. Such an unphysical behaviour stems from defining the quasiparticle energy as the solution of the quasiparticle equation with the largest spectral weight in cases where several solutions can be found. This shortcoming has been thoroughly described in several previous studies.^{78–82} We believe that this central issue

must be resolved if one wants to expand the applicability of the present method.

ACKNOWLEDGEMENTS

PFL and AS thank the European Research Council (ERC) under the European Union’s Horizon 2020 research and innovation programme (Grant agreement No. 863481) for financial support. XB is indebted to Valerio Olevano for numerous discussions. This work was performed using HPC resources from GENCI-TGCC (Grant No. 2019-A0060801738), CALMIP (Toulouse) under allocation 2020-18005, and the CCIPL center

installed in Nantes. Funding from the “*Centre National de la Recherche Scientifique*” is acknowledged. This work has also been supported through the EUR grant NanoX ANR-17-EURE-0009 in the framework of the “*Programme des Investissements d’Avenir*”.

SUPPORTING INFORMATION

See [supporting information](#) for additional potential energy curves computed with other basis sets and within the frozen-core approximation, as well as tables gathering equilibrium distances for smaller basis sets (cc-pVDZ and cc-pVTZ).

* loos@irsamc.ups-tlse.fr

† scemama@irsamc.ups-tlse.fr

‡ ivan.duchemin@cea.fr

§ denis.jacquemin@univ-nantes.fr

¶ xavier.blase@neel.cnrs.fr

- ¹ Runge, E.; Gross, E. K. U. Density-Functional Theory for Time-Dependent Systems. *Phys. Rev. Lett.* **1984**, *52*, 997–1000.
- ² Casida, M. E. In *Time-Dependent Density Functional Response Theory for Molecules*; Chong, D. P., Ed.; Recent Advances in Density Functional Methods; World Scientific, Singapore, 1995; pp 155–192.
- ³ Salpeter, E. E.; Bethe, H. A. A Relativistic Equation for Bound-State Problems. *Phys. Rev.* **1951**, *84*, 1232.
- ⁴ Strinati, G. Application of the Green’s Functions Method to the Study of the Optical Properties of Semiconductors. *Riv. Nuovo Cimento* **1988**, *11*, 1–86.
- ⁵ Albrecht, S.; Reining, L.; Del Sole, R.; Onida, G. Ab Initio Calculation of Excitonic Effects in the Optical Spectra of Semiconductors. *Phys. Rev. Lett.* **1998**, *80*, 4510–4513.
- ⁶ Rohlffing, M.; Louie, S. G. Electron-Hole Excitations in Semiconductors and Insulators. *Phys. Rev. Lett.* **1998**, *81*, 2312–2315.
- ⁷ Benedict, L. X.; Shirley, E. L.; Bohn, R. B. Optical Absorption of Insulators and the Electron-Hole Interaction: An Ab Initio Calculation. *Phys. Rev. Lett.* **1998**, *80*, 4514–4517.
- ⁸ van der Horst, J.-W.; Bobbert, P. A.; Michels, M. A. J.; Brocks, G.; Kelly, P. J. Ab Initio Calculation of the Electronic and Optical Excitations in Polythiophene: Effects of Intra- and Interchain Screening. *Phys. Rev. Lett.* **1999**, *83*, 4413–4416.
- ⁹ Ma, Y.; Rohlffing, M.; Molteni, C. Excited States of Biological Chromophores Studied Using Many-Body Perturbation Theory: Effects of Resonant-Antiresonant Coupling and Dynamical Screening. *Phys. Rev. B* **2009**, *80*, 241405.
- ¹⁰ Puschnig, P.; Ambrosch-Draxl, C. Suppression of Electron-Hole Correlations in 3D Polymer Materials. *Phys. Rev. Lett.* **2002**, *89*, 056405.
- ¹¹ Tiago, M. L.; Northrup, J. E.; Louie, S. G. Ab Initio Calculation of the Electronic and Optical Properties of Solid Pentacene. *Phys. Rev. B* **2003**, *67*, 115212.
- ¹² Palumbo, M.; Hogan, C.; Sottile, F.; Bagalá, P.; Rubio, A. Ab Initio Electronic and Optical Spectra of Free-Base Porphyrins: The Role of Electronic Correlation. *J. Chem. Phys.* **2009**, *131*, 084102.
- ¹³ Rocca, D.; Lu, D.; Galli, G. Ab Initio Calculations of Optical Absorption Spectra: Solution of the Bethe–Salpeter Equation Within Density Matrix Perturbation Theory. *J. Chem. Phys.* **2010**, *133*, 164109.
- ¹⁴ Sharifzadeh, S.; Biller, A.; Kronik, L.; Neaton, J. B. Quasiparticle and Optical Spectroscopy of the Organic Semiconductors Pentacene and PTCDA From First Principles. *Phys. Rev. B* **2012**, *85*, 125307.
- ¹⁵ Cudazzo, P.; Gatti, M.; Rubio, A. Excitons in Molecular Crystals From First-Principles Many-Body Perturbation Theory: Picene Versus Pentacene. *Phys. Rev. B* **2012**, *86*, 195307.
- ¹⁶ Boulanger, P.; Jacquemin, D.; Duchemin, I.; Blase, X. Fast and Accurate Electronic Excitations in Cyanines with the Many-Body Bethe–Salpeter Approach. *J. Chem. Theory Comput.* **2014**, *10*, 1212–1218.
- ¹⁷ Ljungberg, M. P.; Koval, P.; Ferrari, F.; Foerster, D.; Sánchez-Portal, D. Cubic-Scaling Iterative Solution of the Bethe–Salpeter Equation for Finite Systems. *Phys. Rev. B* **2015**, *92*, 075422.
- ¹⁸ Hirose, D.; Noguchi, Y.; Sugino, O. All-Electron GW+Bethe–Salpeter Calculations on Small Molecules. *Phys. Rev. B* **2015**, *91*, 205111.
- ¹⁹ Cocchi, C.; Draxl, C. Bound Excitons and Many-Body Effects in X-Ray Absorption Spectra of Azobenzene-Functionalized Self-Assembled Monolayers. *Phys. Rev. B* **2015**, *92*, 205105.
- ²⁰ Ziaei, V.; Bredow, T. Simple many-body based screening mixing ansatz for improvement of GW/Bethe–Salpeter equation excitation energies of molecular systems. *Phys. Rev. B* **2017**, *96*, 195115.
- ²¹ Refaely-Abramson, S.; da Jornada, F. H.; Louie, S. G.; Neaton, J. B. Origins of Singlet Fission in Solid Pentacene from an ab initio Green’s Function Approach. *Phys. Rev. Lett.* **2017**, *119*, 267401.
- ²² González, L.; Escudero, D.; Serrano-Andrés, L. Progress and Challenges in the Calculation of Electronic Excited States. *ChemPhysChem* **2012**, *13*, 28–51.
- ²³ Loos, P. F.; Scemama, A.; Jacquemin, D. The Quest for Highly-Accurate Excitation Energies: a Computational Perspective. *J. Phys. Chem. Lett.* **2020**, submitted.
- ²⁴ Jacquemin, D.; Duchemin, I.; Blase, X. Benchmarking the Bethe–Salpeter Formalism on a Standard Organic Molecular Set. *J. Chem. Theory Comput.* **2015**, *11*, 3290–3304.
- ²⁵ Bruneval, F.; Hamed, S. M.; Neaton, J. B. A Systematic Benchmark of the *Ab Initio* Bethe–Salpeter Equation Approach for Low-Lying Optical Excitations of Small Organic Molecules. *J. Chem. Phys.* **2015**, *142*, 244101.
- ²⁶ Hung, L.; da Jornada, F. H.; Souto-Casares, J.; Chelikowsky, J. R.; Louie, S. G.; Ogut, S. Excitation Spectra of Aromatic Molecules within a Real-Space GW-BSE Formalism: Role of Self-Consistency and Vertex Corrections. *Phys. Rev. B* **2016**, *94*,

- 085125.
- ²⁷ Hung, L.; Bruneval, F.; Baishya, K.; Ögüt, S. Benchmarking the *GW* Approximation and Bethe–Salpeter Equation for Groups IB and IIB Atoms and Monoxides. *J. Chem. Theory Comput.* **2017**, *13*, 2135–2146.
- ²⁸ Krause, K.; Klopper, W. Implementation of the Bethe–Salpeter Equation in the Turbomole Program. *J. Comput. Chem.* **2017**, *38*, 383–388.
- ²⁹ Jacquemin, D.; Duchemin, I.; Blondel, A.; Blase, X. Benchmark of Bethe–Salpeter for Triplet Excited-States. *J. Chem. Theory Comput.* **2017**, *13*, 767–783.
- ³⁰ Blase, X.; Duchemin, I.; Jacquemin, D. The Bethe–Salpeter Equation in Chemistry: Relations with TD-DFT, Applications and Challenges. *Chem. Soc. Rev.* **2018**, *47*, 1022–1043.
- ³¹ Garcia-Lastra, J. M.; Thygesen, K. S. Renormalization of Optical Excitations in Molecules Near a Metal Surface. *Phys. Rev. Lett.* **2011**, *106*, 187402.
- ³² Blase, X.; Attaccalite, C. Charge-Transfer Excitations in Molecular Donor-Acceptor Complexes Within the Many-Body Bethe–Salpeter Approach. *Appl. Phys. Lett.* **2011**, *99*, 171909.
- ³³ Baumeier, B.; Andrienko, D.; Rohlfing, M. Frenkel and Charge-Transfer Excitations in Donor–Acceptor Complexes From Many-Body Green’s Functions Theory. *J. Chem. Theory Comput.* **2012**, *8*, 2790–2795.
- ³⁴ Duchemin, I.; Deutsch, T.; Blase, X. Short-Range to Long-Range Charge-Transfer Excitations in the Zincbacteriochlorin-Bacteriochlorin Complex: A Bethe–Salpeter Study. *Phys. Rev. Lett.* **2012**, *109*, 167801.
- ³⁵ Cudazzo, P.; Gatti, M.; Rubio, A.; Sottile, F. Frenkel Versus Charge-Transfer Exciton Dispersion in Molecular Crystals. *Phys. Rev. B* **2013**, *88*, 195152.
- ³⁶ Ziaei, V.; Bredow, T. GW-BSE Approach on S1 Vertical Transition Energy of Large Charge Transfer Compounds: A Performance Assessment. *J. Chem. Phys.* **2016**, *145*, 174305.
- ³⁷ Hybertsen, M. S.; Louie, S. G. Electron Correlation in Semiconductors and Insulators: Band Gaps and Quasiparticle Energies. *Phys. Rev. B* **1986**, *34*, 5390–5413.
- ³⁸ Shishkin, M.; Kresse, G. Self-Consistent *GW* Calculations for Semiconductors and Insulators. *Phys. Rev. B* **2007**, *75*, 235102.
- ³⁹ Blase, X.; Attaccalite, C.; Olevano, V. First-Principles *GW* Calculations for Fullerenes, Porphyrins, Phtalocyanine, and Other Molecules of Interest for Organic Photovoltaic Applications. *Phys. Rev. B* **2011**, *83*, 115103.
- ⁴⁰ Faber, C.; Attaccalite, C.; Olevano, V.; Runge, E.; Blase, X. First-Principles *GW* Calculations for DNA and RNA Nucleobases. *Phys. Rev. B* **2011**, *83*, 115123.
- ⁴¹ Rangel, T.; Hamed, S. M.; Bruneval, F.; Neaton, J. B. Evaluating the *GW* Approximation with CCSD(T) for Charged Excitations Across the Oligoacenes. *J. Chem. Theory Comput.* **2016**, *12*, 2834–2842.
- ⁴² Kaplan, F.; Harding, M. E.; Seiler, C.; Weigend, F.; Evers, F.; van Setten, M. J. Quasi-Particle Self-Consistent *GW* for Molecules. *J. Chem. Theory Comput.* **2016**, *12*, 2528–2541.
- ⁴³ Gui, X.; Holzer, C.; Klopper, W. Accuracy Assessment of *GW* Starting Points for Calculating Molecular Excitation Energies Using the Bethe–Salpeter Formalism. *J. Chem. Theory Comput.* **2018**, *14*, 2127–2136.
- ⁴⁴ Levine, B. G.; Ko, C.; Quenneville, J.; Martínez, T. J. Conical Intersections and Double Excitations in Time-Dependent Density Functional Theory. *Mol. Phys.* **2006**, *104*, 1039–1051.
- ⁴⁵ Tozer, D. J.; Handy, N. C. On the Determination of Excitation Energies Using Density Functional Theory. *Phys. Chem. Chem. Phys.* **2000**, *2*, 2117–2121.
- ⁴⁶ Huix-Rotllant, M.; Natarajan, B.; Ipatov, A.; Muhavini Wawire, C.; Deutsch, T.; Casida, M. E. Assessment of Noncollinear Spin-Flip Tamm–Dancoff Approximation Time-Dependent Density-Functional Theory for the Photochemical Ring-Opening of Oxirane. *Phys. Chem. Chem. Phys.* **2010**, *12*, 12811.
- ⁴⁷ Elliott, P.; Goldson, S.; Canahui, C.; Maitra, N. T. Perspectives on Double-Excitations in TDDFT. *Chem. Phys.* **2011**, *391*, 110–119.
- ⁴⁸ Romaniello, P.; Sangalli, D.; Berger, J. A.; Sottile, F.; Molinari, L. G.; Reining, L.; Onida, G. Double Excitations in Finite Systems. *J. Chem. Phys.* **2009**, *130*, 044108.
- ⁴⁹ Sangalli, D.; Romaniello, P.; Onida, G.; Marini, A. Double Excitations in Correlated Systems: A Many-Body Approach. *J. Chem. Phys.* **2011**, *134*, 034115.
- ⁵⁰ Loos, P.-F.; Boggio-Pasqua, M.; Scemama, A.; Caffarel, M.; Jacquemin, D. Reference Energies for Double Excitations. *J. Chem. Theory Comput.* **2019**, *15*, 1939–1956.
- ⁵¹ Furche, F.; Ahlrichs, R. Adiabatic Time-Dependent Density Functional Methods for Excited State Properties. *J. Chem. Phys.* **2002**, *117*, 7433.
- ⁵² Bernardi, F.; Olivucci, M.; Robb, M. A. Potential Energy Surface Crossings in Organic Photochemistry. *Chem. Soc. Rev.* **1996**, *25*, 321.
- ⁵³ Olivucci, M. *Computational Photochemistry*; Elsevier Science: Amsterdam; Boston (Mass.); Paris, 2010; OCLC: 800555856.
- ⁵⁴ Navizet, I.; Liu, Y.-J.; Ferre, N.; Roca-Sanjuan, D.; Lindh, R. The Chemistry of Bioluminescence: An Analysis of Chemical Functionalities. *ChemPhysChem* **2011**, *12*, 3064–3076.
- ⁵⁵ Robb, M. A.; Garavelli, M.; Olivucci, M.; Bernardi, F. A Computational Strategy for Organic Photochemistry. In *Reviews in Computational Chemistry*; Lipkowitz, K. B., Boyd, D. B., Eds.; John Wiley & Sons, Inc.: Hoboken, NJ, USA, 2007; pp 87–146.
- ⁵⁶ Lazzeri, M.; Attaccalite, C.; Wirtz, L.; Mauri, F. Impact of the Electron-Electron Correlation on Phonon Dispersion: Failure of LDA and GGA DFT Functionals in Graphene and Graphite. *Phys. Rev. B* **2008**, *78*, 081406.
- ⁵⁷ Faber, C.; Janssen, J. L.; Côté, M.; Runge, E.; Blase, X. Electron-phonon coupling in the C₆₀ fullerene within the many-body *GW* approach. *Phys. Rev. B* **2011**, *84*, 155104.
- ⁵⁸ Yin, Z. P.; Kutepov, A.; Kotliar, G. Correlation-Enhanced Electron-Phonon Coupling: Applications of *GW* and Screened Hybrid Functional to Bismuthates, Chloronitrides, and Other High-*T_c* Superconductors. *Phys. Rev. X* **2013**, *3*, 021011.
- ⁵⁹ Faber, C.; Boulanger, P.; Attaccalite, C.; Cannuccia, E.; Duchemin, I.; Deutsch, T.; Blase, X. Exploring Approximations to the *GW* Self-Energy Ionic Gradients. *Phys. Rev. B* **2015**, *91*, 155109.
- ⁶⁰ Monserrat, B. Correlation Effects on Electron-Phonon Coupling in Semiconductors: Many-Body Theory Along Thermal Lines. *Phys. Rev. B* **2016**, *93*, 100301.
- ⁶¹ Li, Z.; Antonius, G.; Wu, M.; da Jornada, F. H.; Louie, S. G. Electron-Phonon Coupling from Ab Initio Linear-Response Theory within the *GW* Method: Correlation-Enhanced Interactions and Superconductivity in Ba_{1-x}K_xBiO₃. *Phys. Rev. Lett.* **2019**, *122*, 186402.
- ⁶² Ismail-Beigi, S.; Louie, S. G. Excited-State Forces within a First-Principles Green’s Function Formalism. *Phys. Rev. Lett.* **2003**, *90*, 076401.
- ⁶³ Hohenberg, P.; Kohn, W. Inhomogeneous Electron Gas. *Phys. Rev.* **1964**, *136*, B864–B871.
- ⁶⁴ Kohn, W.; Sham, L. J. Self-Consistent Equations Including Exchange and Correlation Effects. *Phys. Rev.* **1965**, *140*, A1133–A1138.

- ⁶⁵ Parr, R. G.; Yang, W. *Density-Functional Theory of Atoms and Molecules*; Oxford: Clarendon Press, 1989.
- ⁶⁶ Olsen, T.; Thygesen, K. S. Static Correlation Beyond the Random Phase Approximation: Dissociating H₂ With the Bethe-Salpeter Equation and Time-Dependent GW. *J. Chem. Phys.* **2014**, *140*, 164116.
- ⁶⁷ Holzer, C.; Gui, X.; Harding, M. E.; Kresse, G.; Helgaker, T.; Klopper, W. Bethe-Salpeter Correlation Energies of Atoms and Molecules. *J. Chem. Phys.* **2018**, *149*, 144106.
- ⁶⁸ Li, J.; Drummond, N. D.; Schuck, P.; Olevano, V. Comparing Many-Body Approaches Against the Helium Atom Exact Solution. *SciPost Phys.* **2019**, *6*, 040.
- ⁶⁹ Li, J.; Duchemin, I.; Blase, X.; Olevano, V. Ground-State Correlation Energy of Beryllium Dimer by the Bethe-Salpeter Equation. *SciPost Phys.* **2020**, *8*, 020.
- ⁷⁰ Harding, M. E.; Vazquez, J.; Ruscic, B.; Wilson, A. K.; Gauss, J.; Stanton, J. F. High-Accuracy Extrapolated ab Initio Thermochemistry. III. Additional Improvements and Overview. *J. Chem. Phys.* **2008**, *128*, 114111.
- ⁷¹ Furche, F.; Van Voorhis, T. Fluctuation-Dissipation Theorem Density-Functional Theory. *J. Chem. Phys.* **2005**, *122*, 164106.
- ⁷² Maggio, E.; Kresse, G. Correlation energy for the homogeneous electron gas: Exact Bethe-Salpeter solution and an approximate evaluation. *Phys. Rev. B* **2016**, *93*, 235113.
- ⁷³ Furche, F. Developing the Random Phase Approximation Into a Practical Post-Kohn-Sham Correlation Model. *J. Chem. Phys.* **2008**, *129*, 114105.
- ⁷⁴ Toulouse, J.; Gerber, I. C.; Jansen, G.; Savin, A.; Angyan, J. G. Adiabatic-Connection Fluctuation-Dissipation Density-Functional Theory Based on Range Separation. *Phys. Rev. Lett.* **2009**, *102*, 096404.
- ⁷⁵ Toulouse, J.; Zhu, W.; Angyan, J. G.; Savin, A. Range-Separated Density-Functional Theory With the Random-Phase Approximation: Detailed Formalism and Illustrative Applications. *Phys. Rev. A* **2010**, *82*, 032502.
- ⁷⁶ Angyan, J. G.; Liu, R.-F.; Toulouse, J.; Jansen, G. Correlation Energy Expressions from the Adiabatic-Connection Fluctuation Dissipation Theorem Approach. *J. Chem. Theory Comput.* **2011**, *7*, 3116–3130.
- ⁷⁷ Ren, X.; Rinke, P.; Joas, C.; Scheffler, M. Random-Phase Approximation and Its Applications in Computational Chemistry and Materials Science. *J. Mater. Sci.* **2012**, *47*, 7447–7471.
- ⁷⁸ van Setten, M. J.; Caruso, F.; Sharifzadeh, S.; Ren, X.; Scheffler, M.; Liu, F.; Lischner, J.; Lin, L.; Deslippe, J. R.; Louie, S. G.; Yang, C.; Weigend, F.; Neaton, J. B.; Evers, F.; Rinke, P. GW 100: Benchmarking G_0W_0 for Molecular Systems. *J. Chem. Theory Comput.* **2015**, *11*, 5665–5687.
- ⁷⁹ Maggio, E.; Liu, P.; van Setten, M. J.; Kresse, G. GW 100: A Plane Wave Perspective for Small Molecules. *J. Chem. Theory Comput.* **2017**, *13*, 635–648.
- ⁸⁰ Loos, P. F.; Romaniello, P.; Berger, J. A. Green Functions and Self-Consistency: Insights From the Spherium Model. *J. Chem. Theory Comput.* **2018**, *14*, 3071–3082.
- ⁸¹ Veril, M.; Romaniello, P.; Berger, J. A.; Loos, P. F. Unphysical Discontinuities in GW Methods. *J. Chem. Theory Comput.* **2018**, *14*, 5220.
- ⁸² Duchemin, I.; Blase, X. Robust Analytic Continuation Approach to Many-Body GW Calculations. *J. Chem. Theory Comput. (accepted)* **2020**.
- ⁸³ Martin, R. M.; Reining, L.; Ceperley, D. M. *Interacting Electrons: Theory and Computational Approaches*; Cambridge University Press, 2016.
- ⁸⁴ Hedin, L. New Method for Calculating the One-Particle Green's Function with Application to the Electron-Gas Problem. *Phys. Rev.* **1965**, *139*, A796.
- ⁸⁵ Aryasetiawan, F.; Gunnarsson, O. The GW Method. *Rep. Prog. Phys.* **1998**, *61*, 237–312.
- ⁸⁶ Onida, G.; Reining, L.; and, A. R. Electronic Excitations: Density-Functional Versus Many-Body Green's Function Approaches. *Rev. Mod. Phys.* **2002**, *74*, 601–659.
- ⁸⁷ Reining, L. The GW Approximation: Content, Successes and Limitations: The GW Approximation. *Wiley Interdiscip. Rev. Comput. Mol. Sci.* **2017**, e1344.
- ⁸⁸ Hanke, W.; Sham, L. J. Many-Particle Effects in the Optical Spectrum of a Semiconductor. *Phys. Rev. B* **1980**, *21*, 4656.
- ⁸⁹ Strinati, G. Effects of Dynamical Screening on Resonances at Inner-Shell Thresholds in Semiconductors. *Phys. Rev. B* **1984**, *29*, 5718.
- ⁹⁰ Strinati, G. Dynamical Shift and Broadening of Core Excitons in Semiconductors. *Phys. Rev. Lett.* **1982**, *49*, 1519.
- ⁹¹ Dreuw, A.; Head-Gordon, M. Single-Reference Ab Initio Methods for the Calculation of Excited States of Large Molecules. *Chem. Rev.* **2005**, *105*, 4009–4037.
- ⁹² Holzer, C.; Teale, A. M.; Hampe, F.; Stopkowicz, S.; Helgaker, T.; Klopper, W. GW Quasiparticle Energies of Atoms in Strong Magnetic Fields. *J. Chem. Phys.* **2019**, *150*, 214112.
- ⁹³ Hybertsen, M. S.; Louie, S. G. First-Principles Theory of Quasiparticles: Calculation of Band Gaps in Semiconductors and Insulators. *Phys. Rev. Lett.* **1985**, *55*, 1418–1421.
- ⁹⁴ Christiansen, O.; Koch, H.; Jørgensen, P. The Second-Order Approximate Coupled Cluster Singles and Doubles Model CC2. *Chem. Phys. Lett.* **1995**, *243*, 409–418.
- ⁹⁵ Purvis III, G. P.; Bartlett, R. J. A Full Coupled-Cluster Singles and Doubles Model: The Inclusion of Disconnected Triples. *J. Chem. Phys.* **1982**, *76*, 1910–1918.
- ⁹⁶ Christiansen, O.; Koch, H.; Jørgensen, P. Response Functions in the CC3 Iterative Triple Excitation Model. *J. Chem. Phys.* **1995**, *103*, 7429–7441.
- ⁹⁷ Aidas, K. et al. The Dalton Quantum Chemistry Program System. *WIREs Comput. Mol. Sci.* **2014**, *4*, 269–284.
- ⁹⁸ Parrish, R. M.; Burns, L. A.; Smith, D. G. A.; Simmonett, A. C.; DePrince, A. E.; Hohenstein, E. G.; Bozkaya, U.; Sokolov, A. Y.; Di Remigio, R.; Richard, R. M.; Gonthier, J. F.; James, A. M.; McAlexander, H. R.; Kumar, A.; Saitow, M.; Wang, X.; Pritchard, B. P.; Verma, P.; Schaefer, H. F.; Patkowski, K.; King, R. A.; Valeev, E. F.; Evangelista, F. A.; Turney, J. M.; Crawford, T. D.; Sherrill, C. D. Psi4 1.1: An Open-Source Electronic Structure Program Emphasizing Automation, Advanced Libraries, and Interoperability. *J. Chem. Theory Comput.* **2017**, *13*, 3185–3197, PMID: 28489372.
- ⁹⁹ Hättig, C. Structure Optimizations for Excited States with Correlated Second-Order Methods: CC2 and ADC(2). In *Response Theory and Molecular Properties (A Tribute to Jan Lindenberg and Poul Jørgensen)*; Jensen, H. A., Ed.; Advances in Quantum Chemistry; Academic Press, 2005; Vol. 50; pp 37–60.
- ¹⁰⁰ Budzák, Š.; Scalmani, G.; Jacquemin, D. Accurate Excited-State Geometries: a CASPT2 and Coupled-Cluster Reference Database for Small Molecules. *J. Chem. Theory Comput.* **2017**, *13*, 6237–6252.
- ¹⁰¹ Duchemin, I.; Blase, X. Separable Resolution-of-the-Identity with All-Electron Gaussian Bases: Application to Cubic-scaling RPA. *J. Chem. Phys.* **2019**, *150*, 174120.
- ¹⁰² Garniron, Y.; Gasperich, K.; Applencourt, T.; Benali, A.; Ferté, A.; Paquier, J.; Pradines, B.; Assaraf, R.; Reinhardt, P.; Toulouse, J.; Barbaresco, P.; Renon, N.; David, G.; Malrieu, J. P.; Véril, M.; Caffarel, M.; Loos, P. F.; Giner, E.; Scemama, A. Quantum Package 2.0: A Open-Source Determinant-Driven Suite Of Programs. *J. Chem. Theory Comput.* **2019**, *15*, 3591.